Assessment of molecular connectedness in semi-dilute polymer solutions by elongational flow

J. A. Odell, A. Keller and M. J. Miles*
H. H. Wills Physics Laboratory, University of Bristol, Tyndall Avenue, Bristol BS8 1TL, UK

(Received 20 August 1984; revised 26 February 1985)

The study of the response of polymer solutions to purely elongational flow-fields, as assessed by birefringence, has been extended to the semi-dilute region. As the concentration was increased the optical effects seen gave direct indication of the onset of network behaviour above a critical strain-rate. The concentration at which such chain interactions first occur was found to be significantly lower than identified by the conventional c^* criterion. At any given concentration a time scale could be identified below which the system responds as a network and above which, as an assembly of isolated chains. This critical disentanglement time decreased with concentration, consistent with the time needed for overlapping chains to diffuse apart. On a time-scale longer than this disentanglement time, the chains display the same coil–stretch transition with increasing strain-rate as in dilute solutions, with allowance for the increased solution viscosity. On this longer time-scale the chains can slip out of each other's environment, in spite of their geometric overlap. Atactic polystyrene and poly(ethylene oxide) were compared, polystyrene showing the greater entanglement effects by the present criterion. Some reference is made to more strongly interacting systems (H bonds, ionic forces) where chains can only extend in a mutually interacting fashion.

(Keywords: entanglements; elongational-flow; semi-dilute solution; polystyrene)

INTRODUCTION

This paper describes a new experimental approach to entanglements, their identification and characterization, based upon the response of semi-dilute polymer solutions to elongational flowfields.

Entanglement formation is a basic manifestation of flexible long chains responsible for some of the most characteristic behaviour of polymeric matter[1]. In spite of their significance entanglements are most elusive to experimentation and particularly to quantification. Here we present a new approach which provides a method for the assessment and quantification of entanglement effects in solutions.

The present experiments are confined to a chemically simple polymer, polystyrene, with brief reference to poly(ethylene oxide), both of which are available in closely monodisperse form. These are polymers without specific interactions between molecules, the entanglements being essentially due to geometric overlap and Van der Waals forces. Work on molecules with additional polar interactions will be referred to at the end and will form a separate publication at a later date[2].

The new approach arises from a number of studies on chain extension induced by elongational flow, a line of investigation pursued in this laboratory[3-14] and elsewhere[15-18]. These works were originally concerned with low concentrations where the molecules can be considered to be isolated. The relevant parts of these works will first be briefly recapitulated.

Isolated flexible long chains can be virtually fully extended only by flow fields where the extensional component of the velocity gradient dominates over the rotational component[6]. The simplest cases are uniaxial extension or pure shear where the rotational component is zero.

It is expected from theory[19,20] that chain extension within an elongational flow field should set in suddently as the strain rate ($\dot{\varepsilon}$) is continuously increased; at a critical strain rate ($\dot{\varepsilon}_c$) the chain should pass from the slightly distorted random coil to a near fully extended state. The critical strain rate at which extension occurs, is of the order of $1/\tau$, where τ is the lowest order conformational relaxation time of the isolated random coil molecule.

Once the initial resistance of the chain to deformation, as expressed by τ, is overcome the chain will span a larger velocity gradient, hence will become exposed to larger extensional forces, the extension thus becoming a 'run-away' effect. It is important to appreciate that τ is a measure of the response of the unstretched coil to the deforming influence and not a relaxation time associated with the chain in an extended state.

In previous works this predicted sharp coil→stretch transition was verified in dilute solutions of high molecular weight closely monodisperse atactic polystyrene[9,10] and poly(ethylene oxide) (see *Figure 1a*). These experiments enabled the direct assessment of τ of the isolated molecule. τ was found to be a linear function of solvent viscosity, η_0 (*Figure 2*) a result of specific significance for the present work. τ was found to vary with molecular weight (M) as $\tau \propto M^{1.5}$ over the range of solvents investigated.

This behaviour is as expected for a non-free draining coil[21] an expectation which, however, is confined to θ

---

[*] Present address: The Food Research Institute, Colney Lane, Norwich NR4 7UA, UK

0032-3861/85/081219-08$03.00

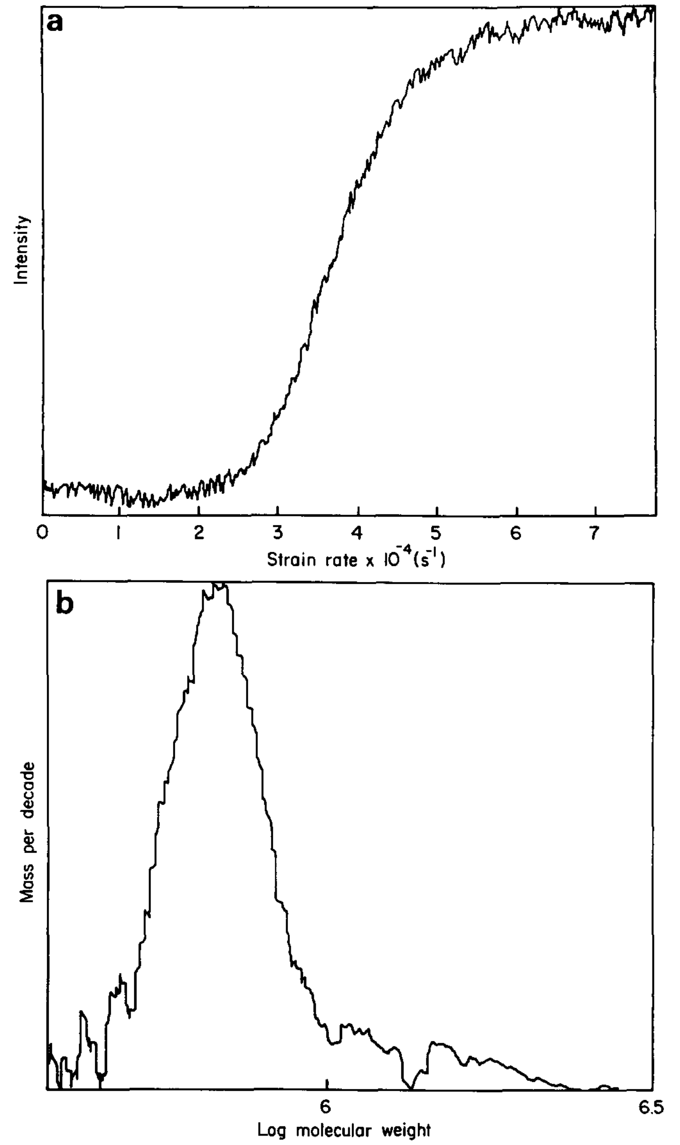

Figure 1 (a) Birefringence *versus* strain-rate in the cross-slots for a 0.1% solution of PEO ($M_w = 1.4 \times 10^6$) in water. (b) The differential molecular weight distribution derived from (a)

conditions, while in our case it is observed to hold also for good solvents at least for high molecular weights.

Even without recourse to theory the experimentally observed relation $\tau \propto M^{1.5}$ was found to be of considerable practical usefulness as it leads to a novel method for determining molecular weight distributions[13]. This fact itself should make it a sensitive tool for detecting any form of interaction between molecules, including mechanically effective entanglements. The present paper, however, will not be concerned with the quantitative subtleties relating to pairing of molecules, which no doubt could also be pursued, but with the advanced stage where an entangled system can be considered as mechanically connected over a macroscopic volume, a stage which is dramatically revealed by our experiment.

EXPERIMENTAL

Principle of method

The method involves the creation of controlled strain-rates by well characterized elongational flow fields and the assessment of chain extension as it occurs within such flow fields. The latter is achieved by observing the birefringence arising from the chain orientation. Qualitatively this involves the visual observation of the onset and the extent of the birefringent region and quantitatively the measurement of the birefringence, which, for the small phase differences involved, is given by the square root of the transmitted intensity between crossed polaroids.

The two elongational flow fields adopted in this work, uniaxial extension and pure shear, were realized by the systems of opposed jets[3] and cross-slots[15] respectively. These flow systems and the experimental methods for producing them have been described previously (see ref. 22).

In the previous experiments with dilute solutions the occurrence of the molecular extension at a critical strain rate ($\dot{\varepsilon}_c$) was signalled by the appearance of a narrow birefringent line along the central outflow axis (as in *Figure 3* from the present work in the case of jets; an analogous bright line appears within the cross-slot region of the slots where it corresponds to a birefringent sheet seen edgewise). Recording of the transmitted intensity of

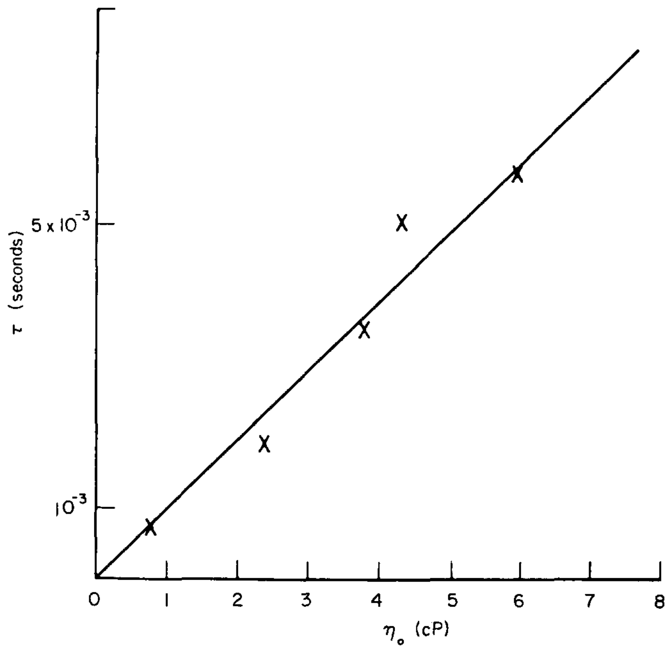

Figure 2 Molecular relaxation time (τ) *versus* solvent viscosity

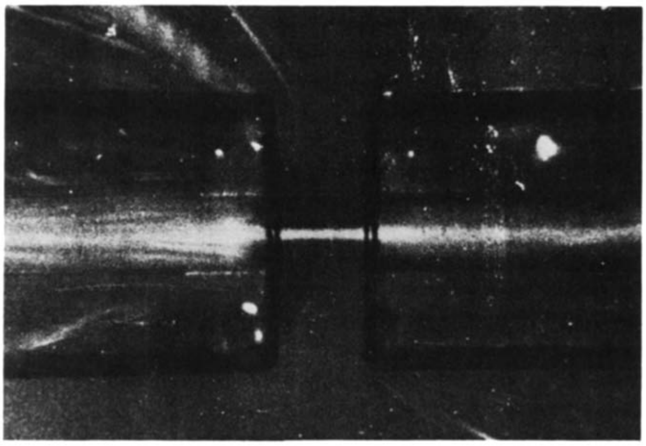

Figure 3 Localized birefringence line passing through the stagnation point in the opposed jets, viewed with polars at 45° to the outlet axis (2.75×10^6 M_w a-PS, 0.1% solution in Dekalin)

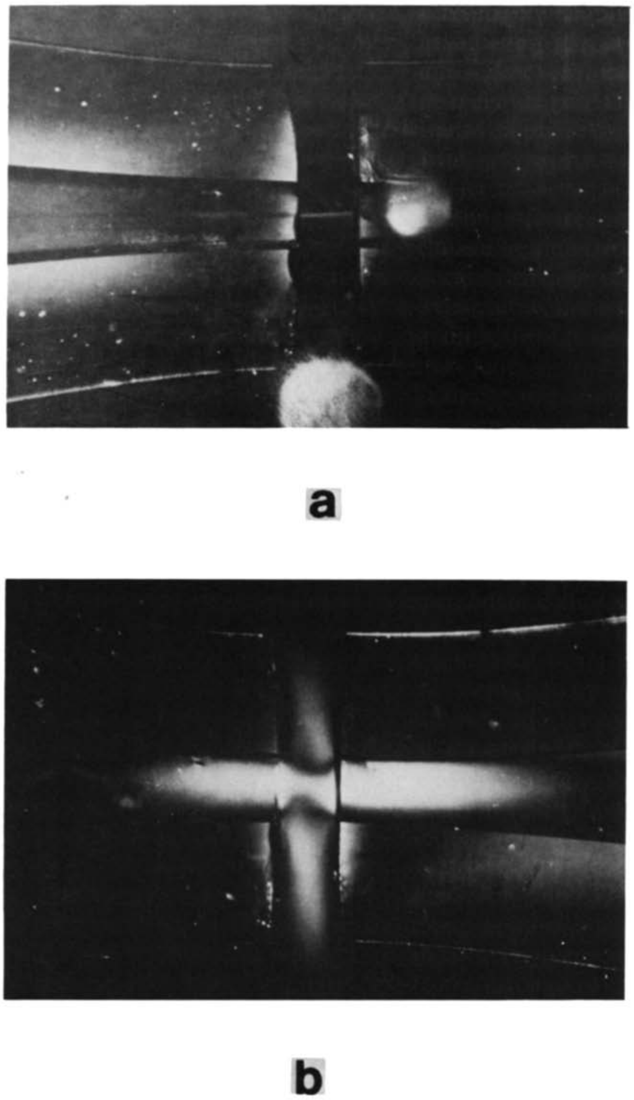

Figure 4 (a) Narrow birefringent line observed between opposed jets in an entangled solution with $\dot{\varepsilon}_c < \dot{\varepsilon} < \dot{\varepsilon}_n$ (0.1%, 7.2×10^6 M_w a-PS in xylene). (b) Flaring of the birefringence in the same solution with $\dot{\varepsilon} > \dot{\varepsilon}_n$

this birefringent line leads to curves such as in *Figure 1* by which $\dot{\varepsilon}_c$, hence τ, can be identified. The latter is done most precisely by differentiation which converts a curve as in *Figure 1a* into a peak as in *Figure 1b*. This after rescaling of the abscissa according to $1/\dot{\varepsilon}_c = \tau \propto M^{1.5}$, corresponds to the differential molecular weight distribution.

For reasons inherent in the way work developed, rather spasmodically over the years, the pictorial representation to follow will be confined to the jet system, while the electronically recorded traces refer to work using the slots; qualitatively similar effects are seen in either system.

The narrowness of the lines, such as in *Figure 3* is central to the present work. This is the consequence of the fact that, in addition to a sufficiently high strain rate also the condition of adequate strain (ε) needs to be satisfied; clearly the strain to which the fluid element is subjected must be sufficiently high for the chain within it to become extended. For example for polystyrene (a-Ps) of 3×10^6 molecular weight, the extension ratio (i.e. contour length to coil diameter) is 200:1; the fluid strain to achieve this will certainly need to exceed this value. The achievement of a large strain requires long enough residence time within the flow field of a given strain rate. This is satisfied for fluid elements passing through or near the point of zero velocity (stagnation point) where they will have the longest residence time. Thus the criterion of high strain will be satisfied only along such stream lines. As in our flow geometries the stagnation points are at the geometric centre of the respective systems, the chain extension will be localized to a narrow region around the central axis, as in fact observed.

It is essential to appreciate the origin of the localization, since it is the break-down of localization that signals the onset of effective entanglements. Thus, as we shall show, we have an indicator of entanglement formation which manifests itself even qualitatively through the change in the shape of the birefringent region apparent even by visual inspection.

RESULTS

Figures 1a and *3*, like all similar traces and photographs in earlier works, were obtained on dilute solutions. It was reported previously that at increased concentration the birefringent zone appeared in the form of a broad bright region, as opposed to the sharp line in *Figure 3*, with unstable boundaries giving the visual impression of bright 'flares', a term by which we shall refer to this effect in what follows. In the earliest report special significance was attached to the purported limiting concentration at a given temperature at which this flare effect set in, which while principally correct, needs to be qualified in the light of information which has emerged since.

Figure 4b displays flares as seen between jets. This was interpreted as due to mechanical interaction between chains, namely that the extending influence of the chains in the centre zone of maximum chain extension is transmitted to other chains which are located beyond the central zone. Accordingly, the chains do not stretch out as they did in isolation but as components of a network which extends over a macroscopic region of the flow field. This comprises the region between the jets (the birefringent line is now broad) and can spread downstream into the jets filling out practically the full jet width, and also spread out upstream outside the jets along the inflow axis where, in the case of dilute solutions, no birefringence is observed. Analogous observations apply to the slots.

It follows that the whole assembly of chains over the birefringent regions must be connected by mechanically

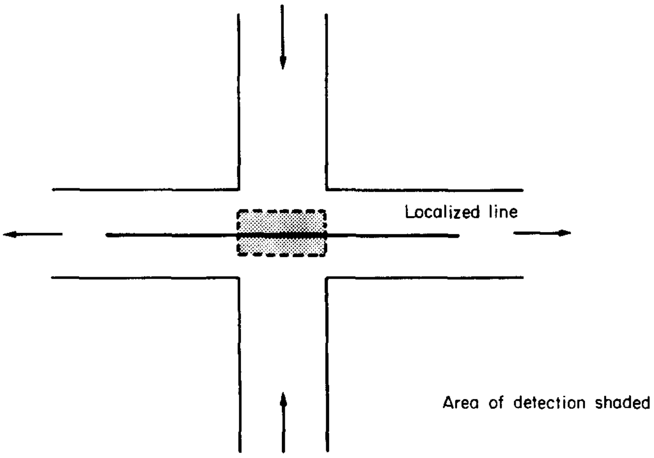

Figure 5 Diagram of the area of detection of the photo-diode between the cross-slots

effective junctions. We shall term these junctions entanglements, without however any implications as regards their specific geometry or topology beyond the undisputed fact that these junctions, whatever their nature, can transmit forces. The flare is an indicator of the existence of such entanglements. Thus we have a simple criterion by which to determine whether the system behaves as a network or as an assembly of isolated chains.

Further exploration reveals, however, that the phenomenon is more subtle and more informative. There is no single concentration above which the system behaves exclusively as a network. Consider again the example of a-PS of 3×10^6 molecular weight at a concentration of say 0.4% where at the appropriate strain rate the flare can be readily observed. Now increase the strain rate gradually from zero.

The first effect seen is the onset of a very narrow birefringent line between the jets at a critical $\dot{\varepsilon}$ value, just as in the case of dilute solutions (*Figure 4a*). As the strain rate is increased beyond this $\dot{\varepsilon}_c$ value the onset of the flare will be observed within a narrow $\dot{\varepsilon}$ interval. *Figure 4b* shows the flare at a highly developed stage. Thus we have two effects at increasing strain rates: (1) at $\dot{\varepsilon}_c$ (as before) the localized narrow birefringent line taken as the extension of isolated chains and (2) at a higher $\dot{\varepsilon}$, to be denoted $\dot{\varepsilon}_n$, the flare sets in, which by the above argument we take as a consequence of extending a network (the subscript denotes network). The sudden onset of extension at $\dot{\varepsilon}_c$ has been the subject of previous communications and is appropriately reflected by the photometer recording of the intensity (*Figure 1a*). It will be important for what follows that the focussed laser beam used for the electronic recording of the trace embraces a rectangular region (as seen in the plane of the image) which is broader than the localized birefringent line as shown diagrammatically in *Figure 5*.

Figure 6 shows intensity *versus* strain-rate curves for a range of concentrations. At the lowest concentration (0.0625%) the curve has the characteristic single step of a dilute solution (as in *Figure 1a*). For concentrations of 0.125% and higher, the curves still show this initial step though with a progressive reduction in $\dot{\varepsilon}_c$ with increasing concentration (indicated by the vertical arrows). Now, however, the flare is registered electronically as a rapid increase in intensity occurring at strain rates beyond the initial step. This is associated with the broadening (hence delocalization) of the initial sharp birefringent line progressively filling the area sensed by the detector (see *Figure 5*).

This increase is not a smooth process but may itself consist of steps. While undoubtedly this structured rise of the intensity must have further information to convey (itself depending on the size of the area chosen for the registration of the intensity) we shall confine ourselves to characterizing it by a single strain-rate parameter. In this we were guided by comparison of the photometric trace with the visual image, where the onset of the 'flare' is seen to appear at a distinctly identifiable $\dot{\varepsilon}$ value ($\dot{\varepsilon}_n$) indicated by the horizontal arrows in *Figure 6*.

We note that with increasing concentration all the curves shift to lower $\dot{\varepsilon}$ values, that is both $\dot{\varepsilon}_c$ and $\dot{\varepsilon}_n$ are decreasing functions of concentration. The same trend is apparent in the corresponding visual images where both the sharp line (*Figure 4a*) and the flare (*Figure 4b*) appear at lower strain rates for higher concentrations.

Throughout the range of concentrations investigated here the extension of chains occurs at lower strain rates than the network effect ($\dot{\varepsilon}_c < \dot{\varepsilon}_n$). We might expect that at higher concentrations entanglement effects will dominate so that the extension of chains might be suppressed by the network effect ($\dot{\varepsilon}_n > \dot{\varepsilon}_c$). Within the scope of the present experiments, however, this 'cross-over' has not been achieved, neither do the presently available data permit extrapolation to such a 'cross-over' point.

Nevertheless we did observe such effects by lowering the temperature. In a single experiment using the same polymer at a concentration of 0.1% the temperature was lowered from 23°C (just above the θ temperature (20°C)) to 18°C (just below the θ temperature). Now the step in the intensity *versus* strain-rate curve does not appear in the trace: instead as the strain-rate increases the transmitted intensity gradually rises (*Figure 7*). Visually this cor-

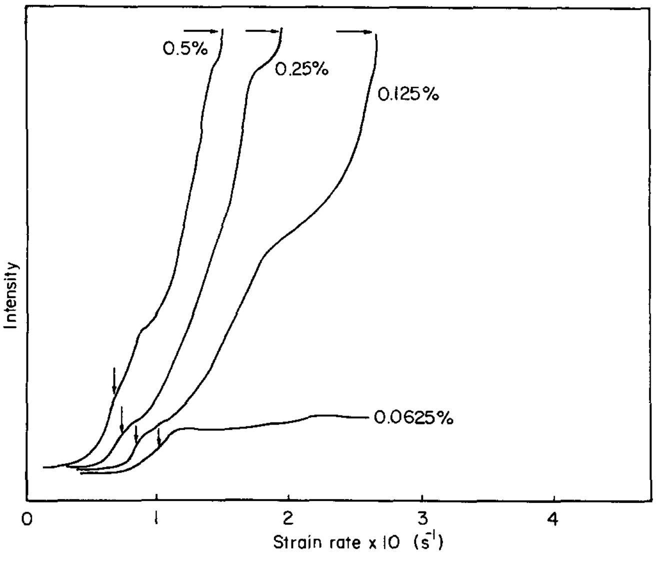

Figure 6 Electronically recorded intensity in the cross-slots *versus* strain-rate for increasing polymer concentration (2.75×10^6 M_w a-PS) in Dekalin. Vertical arrows indicate $\dot{\varepsilon}_c$, and horizontal arrows $\dot{\varepsilon}_n$. Subsequent values of τ and τ_n are derived from such curves

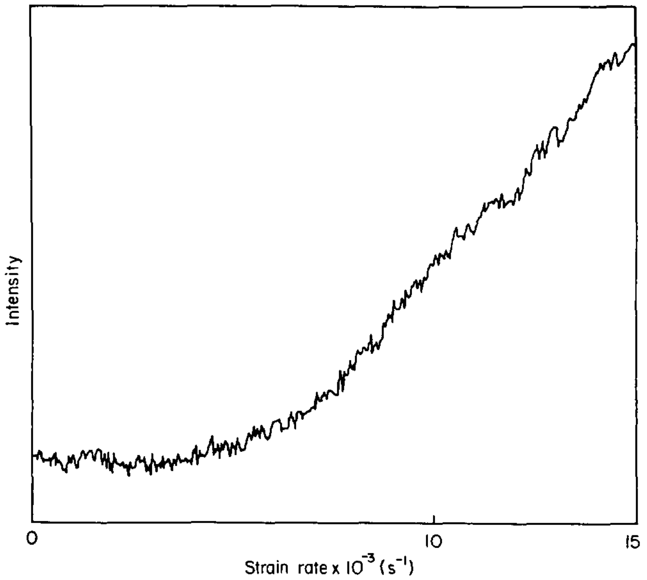

Figure 7 Intensity *versus* strain-rate in the cross-slots below the theta temperature (0.1% solution of 2.75×10^6 M_w a-PS in Dekalin at 18°C)

responds to a gradual development of birefringence ultimately appearing as fully developed flaring, without a preceding localized coil–stretch transition region.

Experiments have been extended to sharp fractions of poly(ethylene oxide) (PEO). The salient observation here is that for identical molecular concentrations and chain lengths considerably higher strain rates are required to produce 'flare' for PEO than for a-PS. Alternatively, for flare to be achieved with PEO by similar strain rates to a comparable fraction of a-PS the concentration needs to be much higher. To illustrate this only one result will be quoted at present: a 0.3% solution of 1.4×10^6 PEO in water produces a coil–stretch transition approximately in agreement with predictions of the Zimm non-free-draining model, but there is no visible flare up to $5\times10^5\ \mathrm{s}^{-1}$, even though on the basis of coil size we expect this solution to possess a degree of overlap similar to a-PS solutions which do show flare. This means that topological entanglements alone cannot characterize the whole entanglement behaviour of a polymer, as the *effectiveness* and lifetime of the entanglements also need to be considered (see below). Further information on PEO will be reported in a separate paper[23].

DISCUSSION

The central effect, the basis of this paper, is the delocalization of the birefringent zone within the flow field in the form of the 'flare' effect. This provides a direct visual registration of the onset of mechanical connectedness and thus serves as a sensitive indicator for mechanically effective entanglements: on a qualitative level for their recognition, and more quantitatively, for their analyses in a simple and direct manner, such as to our knowledge has not been available before. The establishment of the mechanical connectedness by the above criterion is a function of the concentration and strain rate. The first observation is the sudden appearance of the localized birefringent line at a critical strain rate $\dot{\varepsilon}_c$, observable down to extreme dilutions. The second stage characterized by the 'flare' only occurs beyond a certain concentration range at a critical strain rate $\dot{\varepsilon}_n$ where $\dot{\varepsilon}_n > \dot{\varepsilon}_c$, i.e. the flare follows the localized line on increasing $\dot{\varepsilon}$.

Let us reconsider the onset of the localized line (*Figure 4a*). In the dilute solutions of previous works this represented the sudden onset of virtually full chain extension. It will be observed that with increasing concentration this shifts towards lower strain rates (higher τ) (*Figure 6*). A similar dependence of the lowest order relaxation time upon concentration has been previously observed from oscillatory flow birefringence[24]. In *Figure 8* τ is plotted as a function of c. It will be recalled that in highly dilute solutions, where coil overlap was still negligible and the chains could be considered as isolated, τ increased with solvent viscosity η_0 as the solvent was altered for identical concentrations of the same polymer (*Figure 2*). In the present case the solvent is kept the same throughout and it is the solution viscosity which increases with increasing concentration. In *Figure 9* we plot τ against the solution viscosity, both as measured directly with a capillary viscometer and as calculated by the Mark–Houwink equation. Even though there is some scatter of the points, the linear dependence of τ upon solution viscosity is clearly recognizable.

The message of these experiments is now obvious. For a given molecular weight the chains stretch out fully at the critical $\dot{\varepsilon}$ appropriate to the solution viscosity, irrespective of whether the viscosity is primarily determined by the solvent only, as in dilute solution, or whether by the solvent plus solute at the higher polymer concentrations where the polymer significantly affects the viscosity. In other words, even when the polymer concentration is sufficiently high for the chains to overlap, as demonstrated by their ability to transmit their extension to each other (showing the 'flare' effect at high strain rates) on the longer time scale of $\dot{\varepsilon}_c$, the chains will see the other dissolved polymer molecules not as a source of entanglements but as a source of viscous energy dissipation and will extend as if in isolation within a medium of appropriate viscosity. This means that the chains can disentangle and diffuse out of each other's sphere of influence during the time scale relevant for their extension as defined by τ_c.

On the shorter time scale expressed by τ_n ($\tau_n = 1/\dot{\varepsilon}_n$) the overlapping chains are no longer able to slip out of each other's environment, but grip each other, and transmit the extensional force; the whole assembly of partially overlapping chains will act as if connected. τ_n is thus the longest time during which the whole assembly of chains can be regarded as a continuous load bearing network. On a time scale longer than this the chains will slip past each other and will not transmit stress; conversely on an even shorter time scale of $\dot{\varepsilon} > \dot{\varepsilon}_n$, the number of load

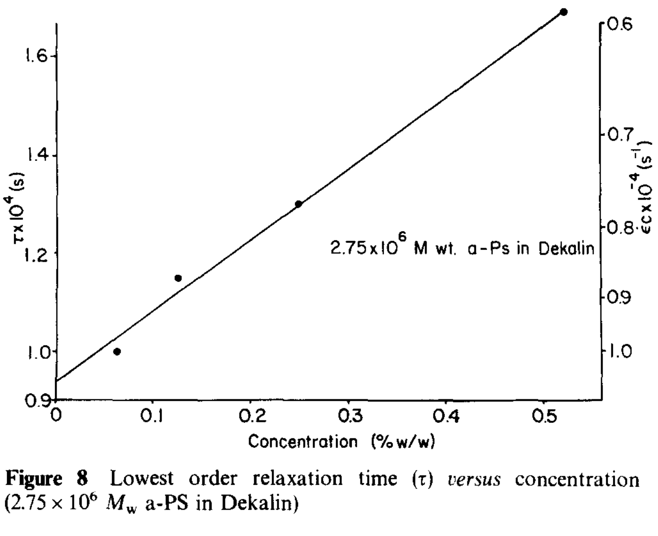

Figure 8 Lowest order relaxation time (τ) *versus* concentration (2.75×10^6 M_w a-PS in Dekalin)

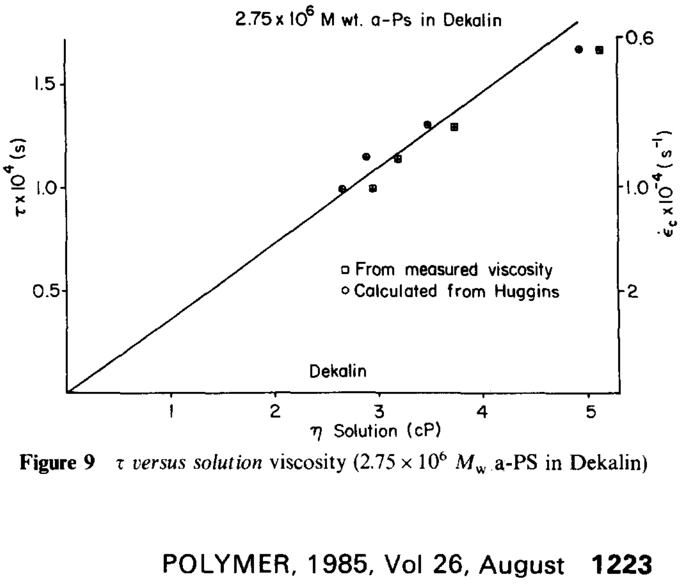

Figure 9 τ *versus solution* viscosity (2.75×10^6 M_w a-PS in Dekalin)

bearing contacts will increase and the network will become stronger. Thus τ_n provides a measure of the limiting disentanglement time and expresses the time scale of the experiment above which the system responds as if entangled and below which as if constituted by isolated chains in a medium of the viscosity corresponding to that of the solution itself. *Figure 10* shows τ_n as a function of concentration.

In what follows we scrutinize the meaning of the two parameters: the critical concentration and the critical time scale.

The concentration

Clearly for coils to be able to interact throughout the system there must be a pathway of mutual contact. In past works the critical concentration at which this pathway establishes itself is expressed by a critical concentration denoted by c^*. This has been calculated in slightly different ways by different authors, on the basis that the chains can be represented as spheres of dimensions defined by the radius of gyration (R_g). c^* then represents the concentration at which contact between spheres is established, or where the mean segment density throughout the solution becomes equal to the mean segment density in the isolated coil. For our system of a-PS with $M = 3 \times 10^6$, the c^* values calculated for the θ condition range from 1 to 5%, depending upon the criterion used.

c^* has been identified experimentally by neutron scattering[25] as corresponding to the concentration where the molecular weight dependence of R_g for dilute solutions ($R_g \propto N^{2/5}$) changes into that predicted for the semi-dilute range ($R_g \propto N^{9/5}$), a distinction valid down to the θ point (or a θ region, see below) but not including the θ point (or region) where this distinction ceases and the relation $R_g \propto N^{1/2}$ will hold irrespective of concentration. These experiments yield a value of the order of 5% for c^* for our material as extrapolated to the θ region.

Other formulations for the critical concentration exist in the literature. Cornet[26] suggests $c^* = 6/[\eta]_\theta$ which, taken together with $[\eta] = KM^{0.5}$ (for the θ state) yields $c^* = 5.3\%$.

At this point we have two comments to make which are closely interrelated. First, that the solid sphere model, traditionally used for defining c^* is a poor approximation of a statistical coil. While it has been adopted for convenience it is often taken too literally. As well recognized, a random coil has no sharp boundary but a segment density gradually decreasing from the centre outwards. It follows that we need to replace the concept of a unique c^* value with the variable parameter of segment overlap density. The different experimental tests based upon, for instance, neutron scattering, viscosity[27] or certain gelation effects[28] adopted for testing interchain contact (hence to establish c^* in the traditional notation) respond to different degrees of this segment overlap (basically determined by their time scale); hence different criteria for overall chain connectivity apply. The fast elongational flow criterion responds more sensitively to small degrees of chain overlap than conventional static tests; it may well be the most sensitive probe for chain continuity known. Mechanically effective continuity can be established on a very short time scale (of the order of 10 μw) down to 0.1% under conditions where the θ state is closely approached. It follows that our results define a limiting contact concentration (c^*) which is less than one tenth of that determined by traditional considerations. The interrelation between time of measurement, disentanglement time and critical overlap segment density is proving to be a fruitful approach in ongoing current works.

We have established, at least qualitatively, that the shorter the time scale upon which we observe the solution, the lower is the concentration at which it behaves as a network. We may ask, given the pseudo-gaussian nature of segment density, whether, with faster experiments, there is any concentration other than that at which the coils are separated by their contour lengths, at which a solution cannot behave as a network. *Figure 10* shows that the curve of τ_n vs. concentration is markedly steepening at 0.1%. A similar effect, though at even lower concentrations (0.01%), has recently been observed in the highly expanded coils of the polyelectrolyte polystyrene sulphonate. We believe that these concentrations represent the 'true' c^* values, below which no network effects are observable, regardless of timescale. This is best interpreted as the point below which the critical criterion of a network (number of associations per coil greater than 2 but less than 3)[29] can no longer be satisfied on any timescale, since the pseudo-gaussian nature of the coils breaks down due to the finite size of the molecule. Further work on this issue is currently in progress.

Critical time

Next we may ask whether the numerical values of the disentanglement times, as expressed by τ_n in *Figure 10*, are realistic or not. Here the diffusion measurements by Leger *et al.* may provide some guidance[30]. These measurements were carried out on stationary systems, applying the ingenious forced Rayleigh scattering method to solutions of sharp fractions of a-PS. We shall not be concerned here with the interpretation by which the results are (successfully) accounted for in terms of reptation theory, but take the actual diffusion coefficients (D) themselves as measured, or extrapolated from the existing data points. In possession of D we can readily calculate the distance over which the molecule would diffuse (x) during a given time (t) as expressed by τ_n in *Figure 10*, through $x = Dt^{1/2}$. The x values thus obtained are shown in *Figure 11*.

There are large error bars associated with the x values which arise from the latitude in the extrapolation of D appropriate to our condition. This, however, does not

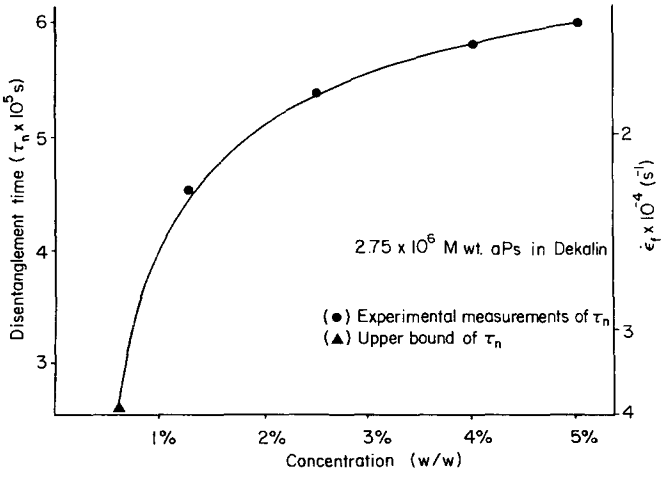

Figure 10 Disentanglement time (τ_n) *versus* concentration (2.75×10^6 M_w a-PS in Dekalin)

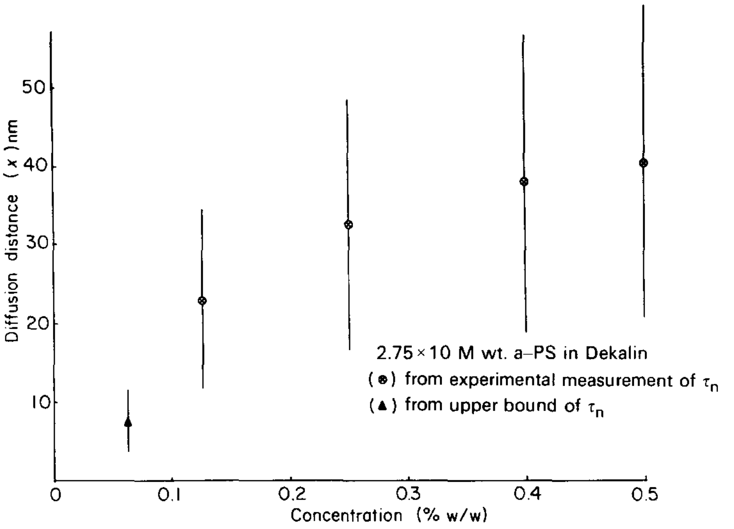

Figure 11 Diffusion distances x calculated from extrapolation of the data of ref. 30 to the molecular weight and τ_n values shown in *Figure 10*. The vertical bars represent the uncertainty in extrapolation

obscure the fact that the x values thus calculated are in the range of the molecular dimensions. The random coil in our material within the θ region (see below) should have a radius of gyration of ≈ 700 Å. The distances involved therefore represent a small to moderate fraction of the coil diameter, increasing with concentration. This is consistent with the picture that the coils overlap by a fraction of their diameter and will behave as isolated chains on extension if they are given the time to diffuse out of each other's environment, a time which we may identify with our disentanglement time. Admittedly this picture of what happens in the course of our postulated disentanglement is necessarily naive, and the justification of the use of D values determined on a static system for our flow experiments may well be questioned. Nevertheless, it is notable that the numbers thus obtained are physically reasonable. Conversely, the fact that transference of D values from a static system to our elongational flow test makes any sense at all is significant in itself, as it implies that it is more the undisturbed diffusion of the still largely unstretched coil, rather than the flow, which is the principal source of the separation of the initially overlapping molecules. In fact, if the figures are taken at face value, the flow itself may have little effect on the disentanglement as such, at least at strain rates not exceeding $\dot{\varepsilon}_n$.

Temperature

A further issue is the temperature. This we did not choose deliberately but used dekalin at the temperature of our laboratory environment which was normally 23°C. We were thus operating just above the ideal θ temperature of mean field theory (20°C)[31] or towards the top of the finite θ region which replaces a discrete θ temperature in tricritical scaling theory[32]. It follows, that we have been justified to regard our system as being at or quite near the θ state as repeatedly invoked in the preceding discussion. A single experiment was performed at the lower limit of the θ region as defined by the tricritical scaling theory (the consequence of a drop in our 'room temperature' in mid winter). As *Figure 7* reveals the consequence of this drop in temperature was dramatic: at this lower temperature (18°C) the chains did not disentangle before the system extends as a continuous network (it only displays the non-localized birefringence developed into a flare). This means that the chains are either more compact and resist chain extension or that the diffusion out of each other's environment is much slower so that the network effect sets in before the coil→stretch transition. When the concentration was reduced below that required to show entanglement effects (0.05%), however, the I vs. $\dot{\varepsilon}$ curve became distinctly different, displaying a clear enough step (even if spread over a wider $\dot{\varepsilon}$ range with lowering of the temperature) for a coil–stretch transition to be identified even down to 16°C, with a progressive reduction in τ reflecting the collapse of the coil below the θ state[22].

This suggests that the flare effect (instead of the sharp localization) setting in at low strain rates in more concentrated solutions below the θ temperature (*Figure 7*) is more likely to be attributable to entanglements where the associations between segments of the different coils have become much stronger so as to prevent disentanglement altogether, an effect seen in other systems with specific associations (for instance hydrogen bonds), see below.

Network formation through specific interactions

In the two polymers used above (a-PS and PEO) no specific interactions are expected between different chains or different portions of the same chain. The entanglement effects therefore should arise essentially through the topology of chain overlap. The fact that $\dot{\varepsilon}_c < \dot{\varepsilon}_n$ is, in part, a consequence of the lack of associations between segments so that segment contact times are short and the different chains behave independently on a time scale longer than $(\dot{\varepsilon}_n)^{-1}$. Even here we found differences between the two polymers. $\dot{\varepsilon}_n$ (PEO) $>$ $\dot{\varepsilon}_n$ (PS) which implies that under comparable conditions of interpenetration the PEO molecules interact more weakly, being more 'slippery' so to speak, and less prone for entanglement formation. Such differences between chains will be much accentuated by the presence of stronger specific interactions. Thus polar forces would be expected to increase the mean time of contact, increasing the disentanglement time and decreasing $\dot{\varepsilon}_n$. In other words we might expect that the overlapping chains will act as a connected network over an increased time interval.

These expectations are well supported by experiments on molecules capable of polar interactions, such as hydrogen bonds or ionic bridges (polyelectrolytes). The results of these experiments will be reported in detail elsewhere[2]. At sufficiently high concentrations such polymers possessing specific associations display the 'flare' as the first and only effect as $\dot{\varepsilon}$ is increased, without the sharp localized line appearing. Specifically, we quote here observations on FM9 (ICI trade name) used as a demisting additive for aerofuel[33]. These molecules are capable of forming intermolecular hydrogen bonds.

Experiments on FM9 were most conveniently conducted in the extensional flow-field of the four-roll mill[2]. In this device we were able to record not only the birefringence effects but also the simultaneously occurring changes in elongational flow viscosity. Solutions of this material show only a 'flare' effect occurring above the critical strain rate $\dot{\varepsilon}_n$. This critical strain-rate is now comparatively low and the onset of flaring is accompanied by a dramatic increase in extensional viscosity. This is

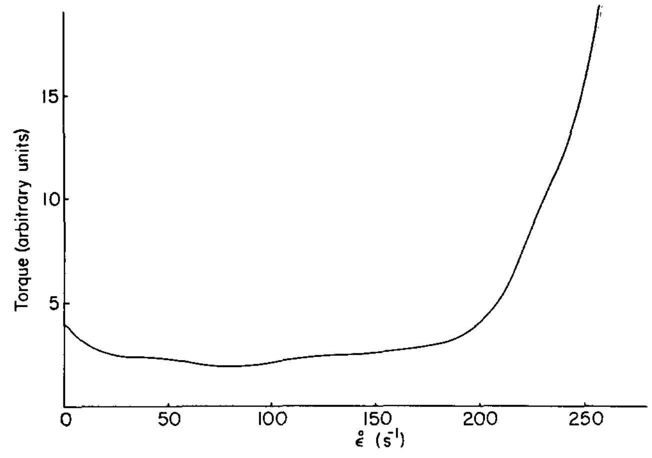

Figure 12 Elongational-flow viscosity in arbitrary units (as measured by the driving torque of the four-roll mill) as a function of strain-rate (0.5% AMK in Dekalin at 23°C)

illustrated on the example in *Figure 12*, where $\dot{\varepsilon}_n$ is of the order of 250 s^{-1}.*

The hydrogen bonding of FM9 can be suppressed by the addition of glacial acetic acid. In this case the solution behaviour resembles that of atactic polystyrene; there exists a critical strain-rate $\dot{\varepsilon}_c$ for the appearance of a localized birefringent line, and the flaring and increase of elongational viscosity at low strain rates are completely suppressed. As before, the limiting time corresponding to $(\dot{\varepsilon}_n)^{-1}$ defines the time scale on which the system can be regarded as connected, which in the instance of $\dot{\varepsilon}_n < \dot{\varepsilon}_c$ acquires the added significance that it will be an expression of the mean life of the polar bonds involved. Thus our technique, in principle, should provide a method for assessing the life time of transient chemical bonds. As a corollary, when $\dot{\varepsilon}_n$ becomes very low, comparable with the time of carrying out a conventional laboratory test, then the system will acquire the characteristics of a permanent network by conventional criteria; in fact it will appear as a gel. Thus 'physical' gelation represents the long time end of the spectrum of transient networks, such as we are presently identifying.

**Figure 12*, chosen from the work on FM9, demonstrates, the main subject of the present paper aside, how experiments recording chain extension in elongational flow fields can be combined with measurement of a macroscopic flow property. Registering of molecular behaviour and rheology simultaneously in the same experiments, is a further potential of our approach which we are currently utilizing.

ACKNOWLEDGEMENTS

We are indebeted to the Science and Engineering Research Council for support throughout the period of the research. We would also like to acknowledge the valuable contribution to the work of Dr K. Tanaka. During the finalization of this work we are pleased to acknowledge the support of the Venture Research Unit of BP International.

REFERENCES

1 Treloar, L. R. G. *Trans. Faraday Soc.* 1940, **36**, 538
2 Odell, J. A. and Keller, A., to be published
3 Frank, F. C., Keller, A. and Mackley, M. R. *Polymer* 1971, **12**, 467
4 Mackley, M. R. and Keller, A. *Philos. Trans. Roy. Soc. London Ser. A* 1975, **278**, 29
5 Crowley, D. G., Frank, F. C., Mackley, M. R. and Stephenson, R. G. *J. Polym. Sci., Polym. Phys. Edn.* 1976, **14**, 1111
6 Frank, F. C. and Mackley, M. R. *J. Polym. Sci. Polym. Phys. Edn.* 1976, **14**, 1121
7 Pope, D. P. and Keller, A. *Colloid Polym. Sci.* 1977, **255**, 633
8 Mackley, M. R. *J. Non-Newtonian Fluid Mech.* 1978, **4**, 111
9 Pope, D. P. and Keller, A. *Colloid Polym. Sci.* 1978, **256**, 751
10 Farrell, C. J., Keller, A., Miles, M. J. and Pope, D. P. *Polymer* 1980, **21**, 129
11 Miles, M. J. and Keller, A. *Polymer* 1980, **21**, 1295
12 Gardner, K., Pike, E. R., Miles, M. J., Keller, A. and Tanaka, K. *Polymer* 1982, **23**, 1435
13 Odell, J. A., Keller, A. and Miles, M. J. *Polymer* 1983, **24** (*Commun.*), 7
14 Miles, M. J., Tanaka, K. and Keller, A. *Polymer* 1983, **24**, 1081
15 Lyazid, A., Scrivener, O. and Teitgen, R. in 'Rheology' (Eds. G. Asterita, G. Marrucci and L. Nicolais), Plenum Pub. Corp., New York, 1980, vol. 2, p. 141
16 Scrivener, O., Berner, C., Cressely, R., Hocquart, R., Sellin, R. and Vloches, N. S. *J. Non-Newtonian Fluid Mech.* 1979, **5**, 475
17 Fuller, G. G. and Leal, L. G. *Rheol. Acta* 1980, **19**, 580
18 Fuller, G. G. and Leal, L. G. *J. Polym. Sci.* 1981, **19**, 557
19 Peterlin, A. *J. Polym. Sci.* (*B*) 1966, **4**, 287
20 De Gennes, P. G. *J. Chem. Phys.* 1974, **60**, 5030
21 Zimm, B. H. *J. Chem. Phys.* 1956, **24**, 269
22 Keller, A. and Odell, J. A. *Colloid Polym. Sci.* 1985, **263**, 181
23 Odell, J. A. and Keller, A., submitted to *J. Polym. Sci. Polym. Phys. Edn.*
24 Lodge, T. P. and Schrag, J. L. *Macromolecules* 1982, **15**, 1376
25 Cotton, J. P., Nierlich, M., Bove, F., Daoud, M., Farnoux, B., Janninck, G., Dupplesix, R. and Picot, C. *J. Chem. Phys.* 1976, **65**, 1101
26 Cornet, C. F. *Polymer* 1965, **6**, 373
27 Aharoni, S. M. *J. Macromol. Sci.--Phys.* 1978, **B15(3)**, 347
28 Tan, H., Moet, A., Hiltner, A. and Baer, E. *Macromolecules* 1983, **16**, 28
29 Eldridge, J. E. and Ferry, J. D. *J. Phys. Chem.* 1954, **58**, 992
30 Leger, L., Hervet, H. and Rondolez, F. *Macromolecules* 1981, **14**, 1732
31 Flory, P. J. 'Principles of Polymer Chemistry' 5th Edn., Cornell University Press, Ithaca, NY, 1966
32 Daoud, M. and Janninck, G. *J. Phys.* (*Paris*) 1976, **37**, 973
33 Peng, S. T. J. and Landel, R. F. *J. Appl. Phys.* 1981, **52**, 5988